

The Hubble time inferred from 10 time-delay lenses

Prasenjit Saha^{1,2}

Jonathan Coles¹

Andrea V. Macciò¹

Liliya L.R. Williams³

ABSTRACT

We present a simultaneous analysis of 10 galaxy lenses having time-delay measurements. For each lens we derive a detailed free-form mass map, with uncertainties, and with the additional requirement of a shared value of the Hubble parameter across all the lenses. We test the prior involved in the lens reconstruction against a galaxy-formation simulation. Assuming a concordance cosmology, we obtain $H_0^{-1} = 13.5^{+2.5}_{-1.3}$ Gyr.

Subject headings: gravitational lensing; cosmological parameters; galaxies: general

1. Introduction

If an object at cosmological distance is lensed into multiple images, the light travel time for individual images differs. For variable sources, the differences are observable as time delays. The delays are of order

$$\Delta t \sim \frac{GM}{c^3} \sim (\Delta\theta)^2 H_0^{-1} \quad (1)$$

where M is the lens mass and $\Delta\theta$ is the image separation (in radians). As Refsdal (1964) first pointed out, the effect provides an independent way of measuring H_0^{-1} . Time-delay measurements have made much progress over the past decade and now at least 15 are available (details below).

¹Institute for Theoretical Physics, University of Zürich, Winterthurerstrasse 190, 8057 Zürich, Switzerland

²Astronomy Unit, Queen Mary and Westfield College, University of London, London E1 4NS, UK

³Department of Astronomy, University of Minnesota, 116 Church Street SE, Minneapolis, MN 55455

While Eq. (1) provides the order of magnitude, to determine the precise factor relating time delays and H_0^{-1} one has to model the mass distribution. An observed set of image positions, rings, magnification ratios, and time delays is generically reproducible by many different mass models. This results in a large model-dependent uncertainty on the inferred Hubble parameter, even with perfect lensing data. To appreciate how serious this model-dependence is, compare the models of B0957+561 by Kundic et al. (1997) and Bernstein & Fischer (1999): the results are $H_0 = 64 \pm 13$ and $77_{-24}^{+29} \text{ km s}^{-1} \text{ Mpc}^{-1}$ respectively, both at 95% confidence; the more general models in the latter paper yield *larger* error-bars. Alternatively, consider the nice summary in Fig. 12 of Courbin (2003) of published H_0 estimates and uncertainties from individual lenses. Among the lenses shown, B1608+656 has all three of its independent time delays measured, B1115+080 has two delays measured, whereas the others have one each. One would expect these two best-measured lenses to be the best constrained. Yet B1608+656 has the largest error-bars on H_0 and B1115+080 the second-largest. This suggests that in the less-constrained lenses the real uncertainties are much larger, but have been underestimated because the fewness of constraints did not force sufficient exploration of model-dependence.

A general strategy for dealing with the non-uniqueness problem is to search through a large ensemble of models that can all reproduce the observations (Williams & Saha 2000; Oguri et al. 2004; Jakobsson et al. 2005). In this paper we will follow such a strategy, simultaneously modeling 10 time-delay lenses coupled by a shared Hubble parameter. The basic method is the same as in Saha & Williams (2004) and the accompanying *PixeLens* code, but a number of refinements have been made.

2. Modeling the lenses

Table 1 summarizes the lenses we have used. By ‘type’ we mean the image morphology (Saha & Williams 2003): AD = axial double, ID = inclined double, SQ = short-axis quad, LQ = long-axis quad, IQ = inclined quad. In B0957+561 two distinct source elements can be identified, both are lensed into ID.

We use *PixeLens* to generate an ensemble of 200 models. Each model in the ensemble consists of 10 pixelated mass maps and a shared value of H_0^{-1} . In addition to reproducing all the observed image positions and time delays, the mass maps are required to satisfy a prior. Errors in the image positions and time delays are assumed negligible, since they are much smaller than the range of models that reproduce the data. The details and justification of the prior are given in Section 2 of Saha & Williams (2004), but basically the mass maps have to be non-negative and centrally concentrated with a radial profile steeper than $|\theta|^{-0.5}$, since

the lenses are galaxies. With one exception the mass maps are required to have 180° rotation symmetry; only B1608+656 is allowed to be asymmetric, because the lens is known to contain two galaxies. A constant external shear is allowed for the lenses where the morphology show evidence of external shear (all except B1608+656, B1104–181, B2149–274). The lensing galaxies in B0957+561 and J0911+055 have cluster environments, but we have not treated these lenses differently. A concordance cosmology with $\Omega_m = 0.3, \Omega_\Lambda = 0.7$ is assumed.

We have not included magnification ratios as a constraint, for two reasons: first, optical flux ratios may be contaminated by microlensing (Keeton et al. 2005) and differential extinction; second, even tensor magnifications—that is, relative magnifications along different directions inferred from VLBI maps—are very weakly coupled with time delays (Raychaudhury et al. 2003), because magnification measures the local second-derivative of the arrival time. Stellar velocity dispersions are available for some of the lenses, but we do not attempt to incorporate them, because current methods for doing so depend on strong assumptions about the mass distribution (Koopmans et al. 2006).

There are five additional candidates we have postponed modeling. B1830–211 has a time delay measurement (Lovell et al. 1998) but the lens position is uncertain (Courbin et al. 2002; Winn et al. 2002). B0909+532 (Ullán et al. 2006) also has an uncertain galaxy position. For B0435–122 (Kochanek et al. 2006) and J1131-123 (Morgan et al. 2006) our preliminary modeling appeared to imply asymmetric lenses, whereas the image morphologies suggest fairly symmetric lenses. Finally, J1650+425 had its time delay measured (Vuissoz et al. 2006) as this paper was being peer-reviewed.

We remark that while *PixeLens* in scientific terms is essentially the same as in Saha & Williams (2004), it has undergone several technical improvements. The key parameter in the code’s performance is the total number of pixels (not pixels per lens) say P . The memory required scales as P^2 and the time scales as P^3 . The maximum usable P is in practice dictated not by time or memory but by the accumulation of roundoff error. Our earlier paper attempted only 3 or 4 lenses at a time, going up to $P \simeq 600$. After improving the control of roundoff error *PixeLens* can now go up to $P \simeq 2000$ and beyond without difficulty. Meanwhile improving the memory management and implementing multi-threading (which parallelizes the computation if run on a shared-memory multi-processor machine) and newer hardware have more than compensated for the P^3 increase in arithmetic.

We have previously done two different tests of the general method. In Saha et al. (2006) the algorithm is tested by feeding time delays sampled from a model ensemble back into *PixeLens* and then recovering the model H_0^{-1} . This showed that any biases introduced by the ensemble-generating process have affected H_0^{-1} by less than 5%, but did not test the prior. Williams & Saha (2000) presented a blind test where one author simulated data using

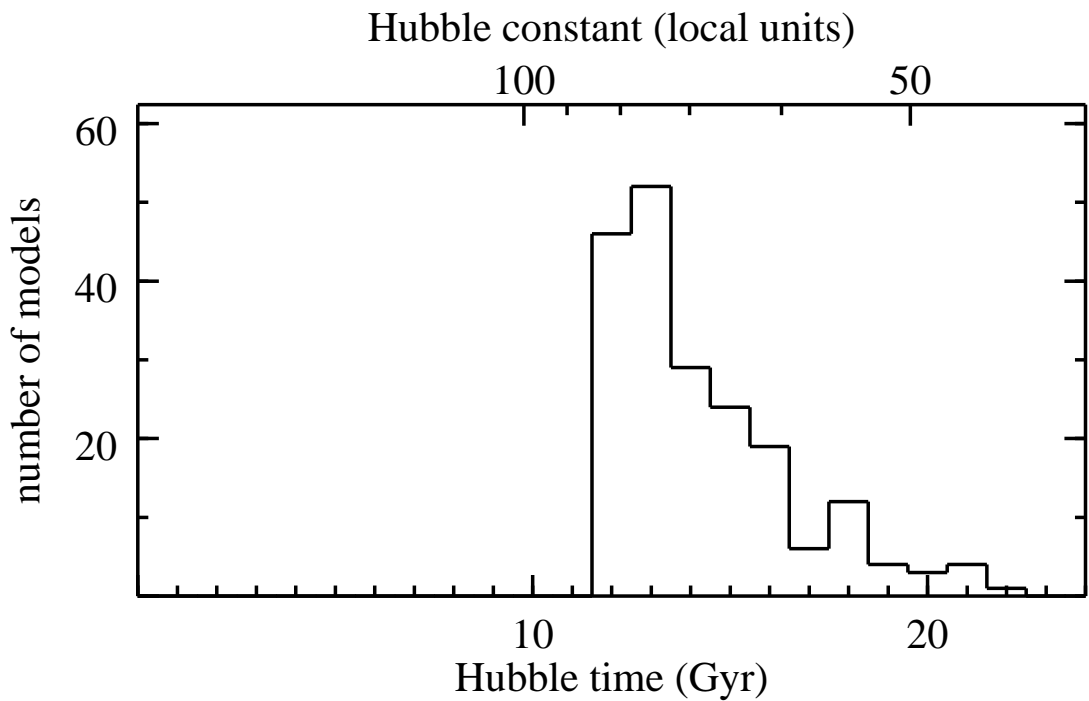


Fig. 1.— Histogram of the ensemble of H_0^{-1} values. The unbinned distribution gives $H_0^{-1} = 13.5_{-1.2}^{+2.5}$ Gyr at 68% confidence and $13.5_{-1.6}^{+5.6}$ Gyr at 90% confidence.

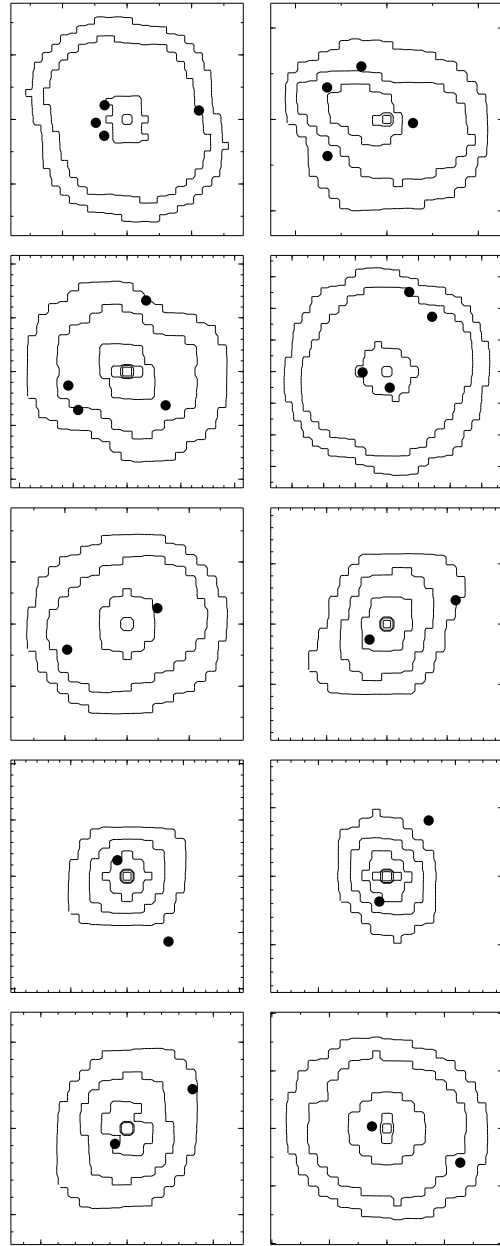


Fig. 2.— Ensemble-average mass maps of the lenses: J0911+055 (upper left), B1608+656 (upper right), B1115+080, B0957+561, B1104-181, B1520+530, B2149-274, B1600+434, J0951+263, B0218+357. The larger tick marks in each panel correspond to $1''$. The contours are in logarithmic steps, with critical density corresponding to the third contour from the outside.

simple model galaxies and a secret fictional value of H_0 , and the other author recovered that value within uncertainties using an ancestor of *Pixelens*. That provided a basic test of the whole procedure, including the prior, but still assumed that the models chosen by the first author for the test were representative of real lensing galaxies. A similar test using current galaxy-formation simulations is desirable but technically formidable; however, we carry out a simple version of such a test below.

3. Results

Our H_0^{-1} distribution is shown in Fig. 1 and may be summarized as

$$H_0^{-1} = 13.5_{-1.2}^{+2.5} \text{ Gyr} \quad (H_0 = 72_{-11}^{+8} \text{ km s}^{-1} \text{ Mpc}^{-1}) \quad (2)$$

at 68% confidence and $13.5_{-1.6}^{+5.6}$ Gyr at 90% confidence. This estimate neglects measurement errors in the time delays. However, we have verified by repeating the analysis with perturbed time delays that the effect of measurement errors is very small. Astrometric errors are also very small.

Fig. 1 is consistent with the analogous Figs. 8 and 11 in Saha & Williams (2004), which derive from 2 time-delay quads and 4 doubles considered separately. But the constraints do not improve as much as simple $1/\sqrt{N}$ would predict. In fact, the uncertainties are far from Gaussian, and some lensing configurations are much more useful than others. Saha et al. (2006) discuss this point in more detail and conclude that a 5% uncertainty on H_0^{-1} is possible using 11 lenses, provided the lenses all have favorable configurations.

Fig. 2 shows ensemble average mass distributions for the 10 lenses. Notice that some lenses, especially B1115+080, B1104–181, and B1520+530, have twisting isodensity contours and/or radially-dependent ellipticities, features that are not included in parametrized models.

The lens galaxies have varying amounts of dark matter. This follows from Ferreras et al. (2005) who compare the total-mass profiles of 18 lensing galaxies, including 6 from the present sample, with stellar-mass profiles from population-evolution models. (The work assumed $H_0^{-1} = 14$ Gyr which is well within our uncertainties, and hence the results are valid for the models here.) From their Table 1 we see that out to $\sim 3R_{\text{eff}}$, B1520+530 is mainly stars, B1115+080, B1608+656, and B2149–274 have significant non-stellar mass, while J0951+263 and B1104–181 are dominated by dark matter.

Table 1: Lenses and time delays

Object	type	z_L	z_S	Δt (days)
J0911+055	SQ	0.77	2.80	146 ± 8^a
B1608+656	IQ	0.63	1.39	$32 \pm 2, 5 \pm 2, 40 \pm 2^b$
B1115+080	IQ	0.31	1.72	$13 \pm 2, 11 \pm 2^{c,d}$
B0957+561	2×ID	0.36	1.41	423 ± 1^e
B1104–181	AD	0.73	2.32	161 ± 7^f
B1520+530	ID	0.71	1.86	130 ± 3^g
B2149–274	AD	0.49	2.03	103 ± 12^h
B1600+434	ID	0.42	1.59	51 ± 4^i
J0951+263	ID	0.24 ^j	1.24	16 ± 2^j
B0218+357	ID	0.68	0.96	$10 \pm 1^{k,l}$

^aHjorth et al. (2002) ^bFassnacht et al. (2002) ^cSchechter et al. (1997) ^dBarkana (1997) ^eOscoz et al. (2001) ^fOfek & Maoz (2003) ^gBurud et al. (2002b) ^hBurud et al. (2002a) ⁱBurud et al. (2000) ^jJakobsson et al. (2005) [photometric z_L] ^kBiggs et al. (1999) ^lCohen et al. (2000)

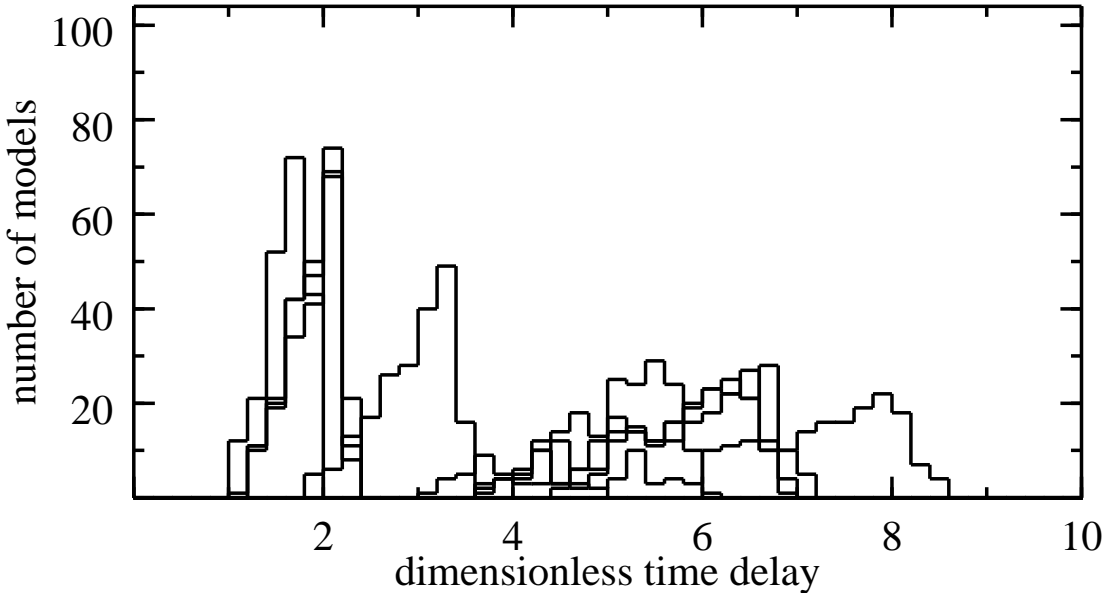


Fig. 3.— Histograms of φ for all ten lenses. J0911+055, B1608+656, B1115+080 all peak around 2. B0957+561 peaks around 3. B1104–181 peaks around 2. B1520+530, B1600+434, J0951+263, B0218+357 all peak around 6. B2149–274 peaks around 8.

4. Lens models compared with a simulation

We now address a simplified version of the question: are our lens models typical of current galaxy-formation simulations?

The details of gas dynamics, star formation, AGN formation, and feedback on galaxy scales are still uncertain. With this caveat in mind, we consider a single high resolution galaxy, extracted from an N -body cosmological simulations and then resimulated using the TreeSPH GASOLINE code (Wadsley et al. 2004) including gas cooling, star formation, supernova feedback and UV background. The galaxy is an E1 or E2 triaxial elliptical with dominated by stars in the inner region but overall $\sim 80\%$ dark matter (Macciò et al. 2006). Orienting this galaxy randomly and ray-tracing with random sources (Macciò 2005) we generated about 500 quads and 10000 doubles, and calculated time delays for each of these.

As Eq. (1) suggests, time delays generated from a single galaxy will range over a factor of only a few, and cannot be directly compared with the observed time delays, which range over a factor of 40. We therefore consider a dimensionless form of the time-delay φ , given by

$$H_0 \Delta t = \varphi \frac{1}{16} (\theta_1 + \theta_2)^2 D \quad (3)$$

where θ_1, θ_2 are the lens-centric distances (in radians) of the first and last images to arrive, Δt is the observed time delay between them, and D is the usual distance factor in lensing. This factors out the dependence of the time delay on cosmology (through H_0 and D) and on the scale of the lens (through $[\theta_1 + \theta_2]^2$), leaving φ dependent only on the shape and steepness of the lens and on the source position with respect to the caustics (Saha 2004).

Fig. 3 shows the histograms of φ in our lens-model ensembles. The quads all peak around 2, while the doubles mostly peak around 5–8; the exceptions are B0957+561 peaking around 3 and B1104–181 peaking around 2. Since B0957+561 is in a cluster, it is plausible that the mass profile is unusually shallow, thus reducing the time delay through the well-known steepness degeneracy. The low value for B1104–181 is more puzzling. Fig. 4 is simpler, showing the probability distributions of φ for doubles and quads generated by the single simulated galaxy.

Figs. 3 and 4 are not quite equivalent, but we can think of both as derived from an underlying $\text{prob}(\varphi|\text{galaxy, lensing obs})$. Each histogram in Fig. 3 weights this probability distribution by observation selection effects and by the *PixeLens* prior, and then marginalizes over galaxies while holding the lensing observables fixed. Fig. 4 marginalizes over lensing observables (separately for doubles and quads) while holding the galaxy fixed. Bearing this difference in mind, the simulated galaxy appears typical of our lens models. The most noticeable difference is the absence of observed quads with φ close to zero; but that is an

expected observational selection effect, because very short time delays are unlikely to be measured.

We conclude that the *PixeLens* prior, as far as this preliminary experiment can reveal, is consistent with galaxy-formation simulations. Further comparisons with simulated galaxies and fine-tuning of the prior are desirable in future work.

5. Discussion

We have expressed our main result (Fig. 1) preferentially in terms of H_0^{-1} rather than H_0 because the former appears more naturally in lensing theory. But it is interesting to continue with H_0^{-1} in comparing with other techniques, because H_0^{-1} has a simple interpretation quite generally: it is a/\dot{a} or the doubling-time for metric distances at the current expansion rate. Coincidentally,¹ in the concordance cosmology ($K = 0, \Omega_m \simeq \frac{1}{4}, w = -1$) H_0^{-1} also equals the expansion age of the universe, within uncertainties. In particular, H_0^{-1} estimates can be immediately compared with globular-cluster ages, such as in Krauss & Chaboyer (2003).

The well-known recent measurements of H_0^{-1} , expressed in Gyr are:

1. 13.6 ± 1.5 from Freedman et al. (2001), who combine several different indicators calibrated using Cepheids;
2. 15.7 ± 0.3 (statistical) ± 1.2 (systematic) from Sandage et al. (2006), using SNIa distances calibrated using Cepheids;
3. 13.6 ± 0.6 from Spergel et al. (2006), using the CMB fluctuation spectrum.

Our result is consistent with any of these.

It is worth noting, however, that the Hubble parameter appears in very different guises in different techniques. The distance-ladder methods measure the local cosmological expansion rate, independent of the global geometry. By contrast, in the CMB, H_0^{-1} is one parameter in a global cosmological model. Lensing is different again: here one assumes a global geometry and then measures a single scale parameter. The same is true of Sunyaev-Zel'dovich and X-ray clusters. The latter technique has made significant progress recently (Jones et al. 2005) but thus far still relies on strong assumptions: spherical symmetry of the cluster potential and hydrostatic equilibrium of the gas. In principle, lensing time delays can determine the

¹Though a spoof paper by D. Scott ([astro-ph/0604011](#)) develops a conspiracy theory for this.

global geometry as well (Refsdal 1966) but the amount of data needed is not observationally viable yet.

Whether lensing time delays can get the uncertainties in the Hubble parameter down to the 5% level is an open question. Maybe galaxy-lens models can be constrained enough to determine H_0^{-1} to better than 5%, thus making lensing the preferred method (Schechter 2004); or maybe the approach is best used in reverse, inputting H_0^{-1} to constrain galaxy structure (Kochanek et al. 2006). Fortunately, either outcome is worthwhile, and the basic technique will be the same. So whether the optimists or the pessimists are right, the usual cliches of “more data!” [time-delay measurements] and “more theory!” [lens models] are both apt.

REFERENCES

Barkana, R. 1997, *ApJ*, 489, 21

Bernstein, G., Fischer, P. 1999, *AJ*, 118, 14

Biggs, A.D., Browne, I.W.A., Helbig, P., Koopmans, L.V.E., Wilkinson, P.N., Perley, R.A. 1999, *MNRAS*, 304, 339

Blandford, R.D., & Kundić, T. 1997, in *The Extragalactic Distance Scale*, ed. M. Livio, M. Donahue, & N. Panagia (Cambridge: Cambridge Univ. Press), 60

Burud, I., et al. 2000, *ApJ*, 544, 117

Burud, I. et al., 2002, *A&A*, 383, 71

Burud, I. et al., 2002, *A&A*, 391, 481

Cohen, A. S., Hewitt, J. N., Moore, C. B. & Haarsma, D. B., 2000, *ApJ*, 545, 578

Courbin, F., Meylan, G., Kneib, J.-P., Lidman, C. 2002, *ApJ*, 575, 95

Courbin, F. 2003, in *Gravitational lensing: a unique tool for cosmology*, eds: D. Valls-Gabaud & J.-P. Kneib, in press. Also available as [astro-ph/0304497](#)

Fassnacht, C. D., Xanthopoulos, E., Koopmans L. V. E. & Rusin D. 2002 *ApJ*, 581, 823

Ferreras I., Saha, P., & Williams L.L.R. 2005, *ApJ*, 623, 5

Freedman, W.L. et al., 2001, *ApJ*, 553, 47

Hjorth, J. et al. 2002, *ApJ*, 572, 11

Jakobsson, P., Hjorth, J., Burud, I., Letawe, G., Lidman, C., Courbin, F. 2005, *A&A*, 431, 103

Jones, M.E. et al., 2005, *MNRAS*, 357, 518

Keeton, C.R., Burles, S., Schechter, P.L., & Wambsganns, J. 2005, *ApJ*, 639, 1

Kochanek, C.S., Morgan, N.D., Falco, E.E., McLeod, B.A., Winn, J.N., Dembicky, J., & Ketzeback, B. 2006, *ApJ*, 640, 47

Krauss, L.M. & Chaboyer, B. 2003, *Science*, 299, 65

Koopmans, L.V.E., Treu, T., Bolton, A.S., Burles, S., & Moustakas, L.A. 2006, [astro-ph/0601628](#)

Kundić, T. et al. 1997, *ApJ*, 482, 75

Lovell, J. E. J., Jauncey, D. L., Reynolds, Wieringa, M.H., King, E.A., Tzioumis, A.K., McCulloch, P.M., Edwards, P.G. 1998, *ApJ*, 508, 51

Macciò, A.V. 2005, *MNRAS*, 361, 1250

Macciò, A.V., Moore, B., Stadel, J., & Diemand, J. 2006, *MNRAS*, 366, 1529

Morgan, N.D., Kochanek, C.S., Falco, E.E., & Dai, X. 2006, [astro-ph/0605321](#)

Ofek, E.O. & Maoz, D. 2003, *ApJ*, 594, 101

Oguri, M. et al. 2004, *ApJ*, 605, 78

Oscoz, A. et al. 2001, *ApJ*, 552, 81

Raychaudhury, S., Saha, P. & Williams, L.L.R. 2001, *AJ*, 126, 29

Refsdal, S. 1964, *MNRAS*, 128, 307

Refsdal, S. 1966, *MNRAS*, 132, 101

Saha, P. 2000, *AJ*, 120, 1654

Saha, P. 2004, *A&A*, 414, 425

Saha, P., Courbin, F., Sluse, D., Dye, S., Meylan, G. 2006, *A&A* 450, 461

Saha, P. & Williams, L.L.R. 1997, *MNRAS*, 292, 148

Saha, P. & Williams, L.L.R. 2003, *AJ*, 125, 2769

Saha, P., & Williams, L.L.R. 2004, *AJ*, 127, 2604

Sandage, A., Tammann, G.A., Saha, A., Reindl, B., Macchetto, F.D., & Panagia, N. 2006, *ApJ*, in press and [astro-ph/0603647](#)

Spergel, D.N. et al., 2006, *ApJ*, in press and [astro-ph/0603449](#)

Schechter, P.L. et al. 1997, *ApJ*, 475, L85

Schechter, P.L. 2004, Proceedings of IAU Symposium No. 225, The Impact of Gravitational Lensing on Cosmology, eds: Y. Mellier & G. Meylan

Ullán, A., Goicoechea, L.J., Zheleznyak, A.P., Koptelova, E., Bruevich, V.V., Akhunov, T., Burkhanov, O., 2006, *A&A*, 452, 25

Vuissoz, C., et al., 2006, [astro-ph/0606317](https://arxiv.org/abs/astro-ph/0606317)

Wadsley, J.W., Stadel, J. & Quinn, T. 2004, *New Astronomy*, 9, 137

Williams, L.L.R. & Saha, P. 2000, *AJ*, 119, 439

Winn, J.N., Kochanek, C.S., McLeod, B.A., Falco, E.E., Impey, C.D., Rix, H.-W. 2002, *ApJ*, 575, 103

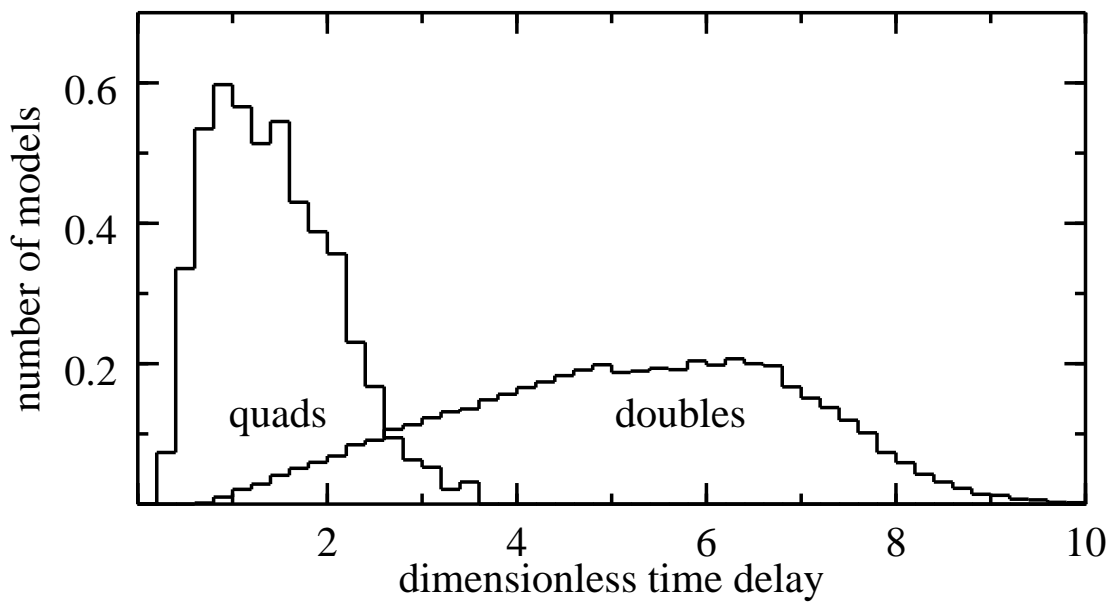


Fig. 4.— Probability distribution of φ for the simulated galaxy. Doubles and quads are normalized separately.